Global and Planetary Change 167 (2018) 46–60

Contents lists available at ScienceDirect

Global and Planetary Change

journal homepage: www.elsevier.com/locate/gloplacha

Research article

Contrasting geometric and dynamic evolution of lake and land-terminating glaciers in the central Himalaya

Owen King[a,*], Amaury Dehecq[b], Duncan Quincey[a], Jonathan Carrivick[a]

[a] School of Geography, University of Leeds, Leeds LS2 9JT, UK
[b] NASA Jet Propulsion Laboratory, Pasadena, CA 91109, USA

ARTICLE INFO

Keywords:
Glacial lakes
Himalaya
Glacial lake outburst floods
Digital elevation model
Glacier velocity

ABSTRACT

The impact of glacial lake development on the evolution of glaciers in the Himalaya is poorly quantified, despite the increasing prevalence of supraglacial and proglacial water bodies throughout the region. In this study we examine changes in the geometry, velocity and surface elevation of nine lake-terminating and nine land-terminating glaciers in the Everest region of the central Himalaya over the time period 2000 to 2015. The land-terminating glaciers we examined all decelerated (mean velocity change of −0.16 to −5.60 m a^{-1} for different glaciers), thinned most in their middle reaches, and developed a more gently sloping surface (−0.02 to −0.37° change) down-glacier over the period 2000–2015. The lake-terminating glaciers we examined all retreated (0.46 to 1.42 km), became steeper (0.04 to 8.68° change), and showed maximum thinning towards their termini, but differed in terms of their dynamics, with one group of glaciers accelerating (mean speed-up of 0.18 to 8.04 m a^{-1}) and the other decelerating (mean slow-down of −0.36 m a^{-1} to −8.68 m a^{-1}). We suggest that these two scenarios of glacier evolution each represent a different phase of glacial lake expansion; one that is accompanied by increasingly dynamic glacier behaviour and retreat, and a phase where glacial lakes have little impact on glacier behaviour that may precede or follow the phase of active retreat. Our observations are important because they quantify the interaction of glacial lake expansion with glacier ice mass loss, and show that increased glacier recession should be expected where a glacial lake has begun to develop.

1. Introduction

The number and size of proglacial (moraine- and ice-dammed) lakes has increased dramatically across the Hindu Kush Karakoram Himalaya (HKKH) in recent decades (Zhang et al., 2015; Nie et al., 2017), and their expansion has been associated with areal and volumetric reductions in glacier extent (Basnet et al., 2013; King et al., 2017; Wang et al., 2017). The presence of a glacial lake may be indicative of a glacier in its most advanced state of recession (Sakai and Fujita, 2010; Benn et al., 2012), thus glacial lakes may become populous in high mountain regions as precipitation and temperature changes continue. Glacial lakes are particularly likely to form where substantial moraine dams have been constructed during glacial maxima (Benn et al., 2012). Ice mass loss rates from marine- and lake-terminating glaciers have been shown to be elevated above their land-terminating counterparts elsewhere in the world (Truffer and Motyka, 2016; Willis et al., 2012; McNabb and Hock, 2014; Tsutaki et al., 2016; Melkonian et al., 2016), and their flow characteristics have been found to be contrasting (Willis et al., 2012; Burgess et al., 2013). If simulations of Himalayan glacier evolution over coming decades are to be robust, it is therefore imperative that we improve our understanding of the response of Himalayan glaciers to glacial lake growth.

At present, knowledge of Himalayan glacial lakes and their impact on the dynamics of their host glaciers remains relatively limited. Nie et al. (2017) documented 2.7, 51.7 and 366.6% increases in the total area of glacier fed but unconnected, proglacial and supraglacial lakes, respectively, between 1990 (n = 4549) and 2015 (n = 4950) across the entire HKKH. Reynolds et al. (2000), Quincey et al. (2007), and Sakai and Fujita (2010) identified a set of glacier surface characteristics conducive to supraglacial lake formation. They suggested that meltwater ponding and pond coalescence is most likely where the glacier surface has a surface gradient of < 2° and a negligible velocity, with steeper, faster glacier surfaces liable to meltwater runoff and/or fracturing that would promote meltwater drainage. Thakuri et al. (2016) examined the evolution of one lake-terminating glacier in the Everest region- Imja Tsho, showing an increased surface lowering rate, but decreased surface velocity over Imja and Lhotse Shar Glaciers between 2001 and 2014 and 1992/93 to 2013/14, respectively. King et al.

* Corresponding author.
E-mail address: gy08ok@leeds.ac.uk (O. King).

https://doi.org/10.1016/j.gloplacha.2018.05.006
Received 16 November 2017; Received in revised form 11 May 2018; Accepted 15 May 2018
Available online 24 May 2018

(2017) generated glacier mass balance estimates for 32 glaciers in the Everest region of the Himalaya over the period 2000 to 2015 and showed 32% greater mass loss from lake-terminating glaciers when compared with land-terminating glaciers. King et al. (2017) also show amplified surface lowering rates and opposing surface lowering gradients over lake versus land-terminating glaciers.

Glacial lakes present a considerable societal hazard to communities downstream due to their susceptibility to catastrophic drainage and the release of a glacial lake outburst flood (GLOF) (Fujita et al., 2013). Carrivick and Tweed (2016) compiled a record of 216 glacier flood events from 78 different sites in central Asia (since ~1500 CE) and ranked central Asian countries as most susceptible in a damage index considering recorded deaths, evacuations, and property and infrastructure destruction and disruption. In a region-wide study of glacial lake growth in the Himalaya, Nie et al. (2017) identified 118 rapidly expanding lakes that may be a priority for risk assessment. Rounce et al. (2017) identified 131 glacial lakes in Nepal with an area of > 0.1 km^2, and attempted to categorise glacial lakes based on their outburst probability, and considered the effects of lake expansion on the likelihood of lake failure. Rounce et al. (2017) classified 11 'very high risk' lakes and 31 'high risk' lakes. Rounce et al. (2017) identified Imja Tsho (in the Everest region) as a lake that will become increasingly hazardous, citing lake expansion towards more avalanche prone terrain as the primary factor increasing the chance of an outburst flood occurring. Using an alternative hazard assessment framework, ICIMOD (2011) identified 49 hazardous, and 21 critically hazardous glacial lakes (out of 1466) in Nepal. Concern over the hazard posed by glacial lakes has seen major remediation efforts to stabilise moraine dams and lower lake levels at several sites in recent decades (Reynolds et al., 2000; Rounce et al., 2017), underlining the importance of understanding their likely evolution as climate in the region continues to change (Sakai and Fujita, 2010; Yang et al., 2011; Salerno et al., 2015).

In this study we examine the evolution of nine lake-terminating and nine land-terminating glaciers in the Everest region of the central Himalaya, which is a region that has experienced a 20% increase in lake area from 2000 to 2009 (Gardelle et al., 2011). The primary research question we pose is whether changes in glacier velocity, geometry, and rates of mass loss over the period 2000 to 2015 differ based on terminus type. We use observations of surface dynamics and morphology to examine the processes that may be driving glacier change in this region. Finally, we demonstrate how these data can be used to highlight glaciers that are preconditioned for glacial lake formation or lake expansion in the imminent future.

2. Study area

Glaciers of the Everest region (Fig. 1) can be broadly grouped into three categories:

1. Large land-terminating glaciers flowing down from mountain massifs such as Everest, Lhotse, Cho Oyu and Makalu (all > 8000 m a.s.l.) that terminate on land and account for the greatest portion of glacierised area. These glaciers vary in length, ranging from 1 to 2 km to > 10 km long. These glaciers are flanked by large Little Ice Age (LIA) moraines and are mantled by debris layers up to several metres in thickness (Nakawo et al., 1986, 1999).

2. Lake-terminating glaciers that vary in size and surface cover. Lake areas vary from < 1 km^2 to nearly 4 km^2, debris-cover ranges from 0 to 100%, and glacier length ranges from 3 to 12 km. The majority of glacial lakes are proglacial, although large supraglacial lakes have recently developed on Rongbuk and Drogpa Nagtsang glaciers (Fig. 1).

3. Numerous smaller, clean ice glaciers located at high elevation (> 5000 m a.s.l.), mostly north of the orographic divide in the Everest region. These glaciers do not typically host glacial lakes and have only retreated a small amount from their LIA limits. We do not focus on glaciers of this type in this study.

The nine glaciers we classify as lake-terminating are Imja/ Lhotse Shar, Yanong, Yanong North, Kada, Drogpa Nagtsang, Trakarding, Longmojian, Duiya and Hunku glaciers (Fig. 1, Table S1). These glaciers all have well-developed glacial lakes which are dammed by a full moraine loop, and lose mass through calving as well as melt (Benn et al., 2001; Somos-Valenzuela et al., 2014). We do not classify glaciers that host supraglacial lakes as lake-terminating as we cannot be certain of the depth of these lakes and whether they are directly influencing glacier behaviour. The nine land-terminating glaciers we assess are G1, Erbu, Tibet 1, Ayi, Gyabrag, Rongbuk, Rongbuk East, Khumbu and Lhotse glaciers (Fig. 1). Glacier attributes for both lake- and land-terminating glaciers can be found in Supplementary Table 1.

3. Methods and data

3.1. Data sources

Glacier surface velocity data were generated by tracking surface features in a series of Landsat 7 (ETM+) and 8 (OLI) panchromatic images (both 15 m spatial resolution) (c.f. Dehecq et al., 2015). First, individual displacement fields were generated at 120 m resolution for all pairs of images separated by approximately 1 year (between 352 and 384 days) using orientation correlation (Fitch et al., 2002) with a correlation window of 16 × 16 pixels, and divided by the pair time span to derive as close to annual velocity fields as the imagery archive allows. Second, velocity fields for a similar period of time were stacked together by taking the median value of the velocity stack in each pixel. For this study, stacks of velocity fields were generated for the period 1999 to 2003 (Landsat ETM+) and 2013 to 2015 (Landsat OLI). Uncertainty is estimated at each pixel based on the number and median absolute deviation of the velocity estimates, using a relationship that is calibrated using off-ice measurements (Dehecq et al., 2015). The median uncertainty associated with velocity measurements is ± 1.93 (1999/03) and ± 1.22 (2013/15) m a^{-1} over stable, off-glacier areas and ± 2.71 (1999/03) and ± 1.61 (2013/15) m a^{-1} over glacier surfaces.

Glacier surface lowering and glacier geometry data were derived from the DEM time series presented in King et al. (2017). DEMs in this time series included the Shuttle Radar Topographic Mission (SRTM) 1 arc *sec* DEM and multiple Surface Extraction with TIN-based Searchspace Minimization (SETSM) derived DEMs produced by Ohio State University and distributed online by the Polar Geospatial Center at the University of Minnesota following the approach of Noh and Howat (2015). The SRTM DEM was generated by interferometry using data acquired in February 2000, and the SETSM photogrammetric DEMs were generated from optical stereo (WorldView, 1, 2 and 3) imagery spanning the period 15/01/2014 to 04/05/2015. Previous studies have suggested that the SRTM dataset may underestimate glacier surface elevations because of the penetration of C-band radar waves into snow and ice (Rignot et al., 2001). To account for this bias, we generated a clean ice, firn and snow cover mask using a Landsat ETM+ scene (05/01/2002) acquired close to the date of the SRTM, and applied elevation corrections of +4.8 m over areas of firn/snow, +1.2 m over areas of clean ice and no correction over debris covered glacier surfaces, following the approach of Kääb et al. (2012) and King et al. (2017). The two DEM sets were coregistered following the approach of Nuth and Kääb (2011) where geolocation errors, along or cross track tilts and elevation dependant biases were corrected for, if present. King et al. (2017) give a thorough description of the DEM coregistration and correction process, along with the methods used to estimate surface elevation change uncertainty budgets. The estimated uncertainty (standard error over off-glacier areas) associated with elevation change data is glacier dependant due to area (glacier hypsometry) weighting, but ranges from ± 0.14 to ± 0.39 m a^{-1}.

Additional datasets included the Randolph glacier inventory (RGI) version 5.0 (Bajracharya et al., 2014) and Level-1 terrain processed Landsat imagery from Landsat TM, ETM+ and OLI sensors. A full scene

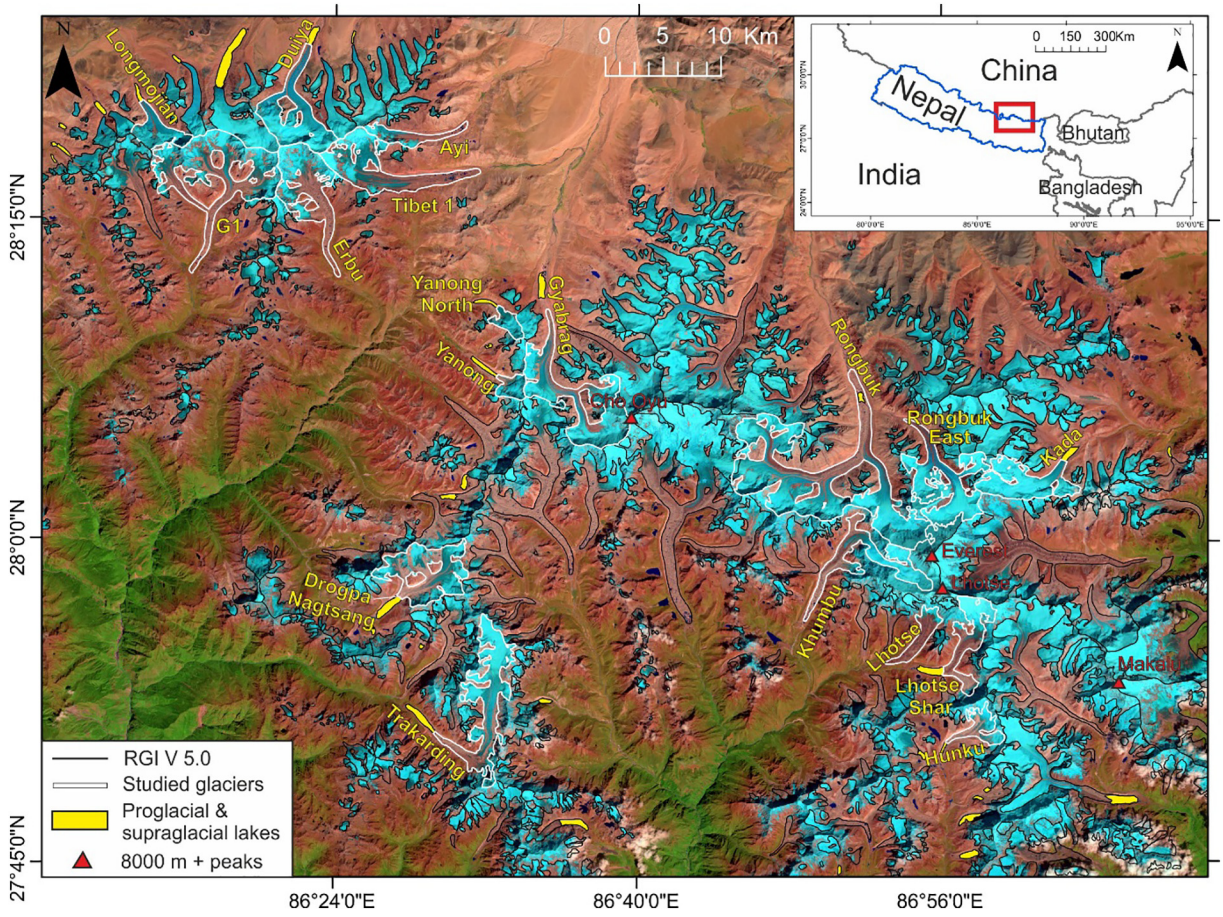

Fig. 1. The Everest region of the central Himalaya. Black glacier outlines show the extent of the RGI version 5.0, whereas white glacier outlines mark the glaciers we focus on in this study. Pro- and supraglacial lakes are also marked, along with mountain peaks above 8000 m in the area. Background imagery is a Landsat OLI image from 2014 available from http://earthexplorer.usgs.gov/.

list is included in supplementary information (Table S2). RGI data provided glacier extent information for clipping of glacier surface elevation and glacier surface velocity data. Landsat TM, ETM+ and OLI archive data were used to document lake-terminating glacier ice front locations over the period 1989–2015.

3.2. Glacier surface geometry assessment and glacier velocity profiles

In contrast to previous studies, which have either measured surface slope from a fixed point at the glacier terminus (e.g. Quincey et al., 2007), or from a fixed point at the front of a distance bin (Miles et al., 2016), we chose to fit a line through 'average' glacier surface elevation profiles over 750 m bin lengths. 'Average' surface elevation profiles were calculated as the mean surface elevation taken from manually delineated flow-parallel profiles spaced 100 m apart, including the glacier centreline (n = 3 or 5 depending on glacier width) across the glacier surface (see Fig. S1 for an example). The comparison of slope estimates from a variety of bin lengths (250, 500, 750, and 1000 m) showed 750 m to be the ideal bin length that characterised general undulations in glacier surface topography; shorter or longer bin lengths produced noisy or artificially smoothed glacier surface gradient estimates, respectively (Fig. S2).

We followed a similar flow line average approach to summarise glacier velocity data over the study period (Fig. S1). Again, we calculated mean glacier velocity from flow-parallel profiles spaced 100 m apart across the glacier surface. This approach was preferred to using a centreline velocity in isolation as this cannot account for cross-glacier fluctuations caused by drag at the ice margins. We applied this approach to both velocity stacks (1999 to 2003 and 2013 to 2015) to allow the calculation of velocity differences over the study period.

We limited our analysis of glacier geometry change and surface velocity fluctuations to below the median altitude of each glacier, which we have used as a proxy of the equilibrium line altitude (ELA) (Braithwaite and Raper, 2009), as the impact of lake development is likely to be most profound in this part of each glacier (Sakai et al., 2015). This approach also limited analyses to areas where data quality was highest, with DEM extraction and feature tracking performing poorly in areas of low-contrast and textureless terrain, such as snow-covered glacier accumulation zones.

3.3. Glacier front position delineation

The calving fronts of lake-terminating glaciers were delineated manually from scenes contained in the Landsat TM, Landsat ETM+ and Landsat OLI archives using ArcMap GIS software. We mapped ice front positions over the period 1989 to 2015 (Table S2). Variations in frontal position were calculated following the box method proposed by Moon and Joughin (2008), where average front position change is derived by

dividing the total area of a polygon including the calving front by the width of a fixed reference profile in the up-glacier direction. Glacial lake area was attained following the approach of studies such as Nie et al. (2017) to classify water bodies in Landsat TM, ETM+ and OLI scenes using the Normalised Difference Water Index.

The uncertainty associated with the measurement of the position of a glacier front using repeat imagery is composed of image co-registration error and delineation errors (Ye et al., 2006). We follow the method of Ye et al. (2006) to estimate glacier front position uncertainty, incorporating the pixel resolution (30 m for Landsat TM and 15 m for Landsat ETM+ and Landsat OLI scenes) and registration error, taken as the Geometric Root Mean Square Error (GRMSE) value provided in the image metadata, into the error budget. Consequently, uncertainty in calculating the mean front position change was ± 0.008 km a^{-1} across all epochs, ranging from ± 0.002 to ± 0.018 km a^{-1} for different time periods and across different image pairs. We followed the approach of Fujita et al. (2009) to estimate the uncertainty associated with glacial lake area, and assume that the perimeter of the glacial lake has been identified to within ½ a single pixel. Mean lake area uncertainty across all time periods and scenes was ± 0.08 km^2, and ranged from ± 0.04 to ± 0.19 km^2 depending on scene resolution.

3.4. Debris cover extent mapping

To quantify the extent of debris cover over our sample of glaciers we first generated a clean ice, firn and snow mask using a Landsat OLI scene and band ratio ($\left(\frac{\text{OLI Band 4}}{\text{OLI Band 6}}\right)$ and a manually set threshold) techniques following the approach Paul et al. (2016). We then used this mask to eliminate non-debris covered glacier areas from the RGI inventory, leaving a mask of only debris-covered glacier area.

4. Results

4.1. Glacier geometry and glacier geometry change

All land-terminating glaciers exhibited a reduction in surface slope values in the down-glacier direction and therefore have a concave surface profile (Figs. 2 and 3). The surface slope did not exceed 8° in any case below ELAs, and 5 of the 9 glaciers we assessed had large portions of < 2° slope. All of the land-terminating glaciers showed a distinct trend in surface gradient change. The upper reaches of the ablation zone of land-terminating glaciers steepened, whilst the gradient of their lower reaches reduced (Figs. 2 and 3). The transition from slight surface steepening to surface gradient reduction occurred at or close to the zone where debris cover became prevalent on each glacier. Mean surface gradient change was effectively zero as a result (−0.03° across the nine glaciers), but ranged from +1° (Rongbuk East and Ayi glaciers) to −4° (Gyabrag Glacier).

Five of the nine lake-terminating glaciers showed increasing surface slope down glacier and thus exhibited a convex down-glacier profile (Figs. 4 and 5). The remaining four lake-terminating glaciers showed either a linear or concave-down profile. Broadly speaking, lake-terminating glaciers were steeper than land-terminating glaciers, with some showing sections of > 20° slope. The style of geometry change shown by lake-terminating glaciers contrasted with that of land-terminating glaciers. Of the nine lake-terminating glaciers we studied, 5 showed pervasive increases in surface gradient throughout the length of their ablation zones (glaciers shown in Fig. 4). A mean of 1.37° of surface steepening occurred over these 5 glaciers (ranging from 0.33 to 2.35° for individual bins). Surface steepening was most substantial within 1 to 2 km of glacier calving fronts. Slight glacier surface steepening (mean 0.25°) occurred on the other four lake-terminating glaciers we assessed (Drogpa Nagtsang, Hunku, Longmojian and Trakarding glaciers; Fig. 5), and they displayed the same down-glacier trend in geometry change as the land-terminating glaciers.

4.2. Glacier velocity and glacier velocity change

Large portions of land-terminating glaciers were either stationary or flowing at a rate below the level of detection of the feature tracking algorithm (Figs. 2 and 3). Across the nine land-terminating glaciers, a mean of 37% of their total length was flowing at or < 4 m a^{-1}. In contrast, seven of the nine lake-terminating glaciers showed active flow throughout their length, with Drogpa Nagtsang and Trakarding glaciers being the exceptions to this rule. Lhotse Shar Glacier showed little to no flow around its calving front between 1999 and 2003, but showed velocities of ~10 m a^{-1} in the 2013 to 15 velocity stack over the same area. Those lake-terminating glaciers that do show active flow throughout were flowing as fast at their terminus as at the approximate ELA.

Comparison of the two velocity stacks (from 1999 to 2003 and from 2013 to 2015) revealed substantial changes in ice velocities over the study period. Land-terminating glaciers decelerated over large portions of their lower reaches (Figs. 2 and 3). Mean, ablation zone velocity reduction was −2.31 m a^{-1} (ranging from −0.16 m a^{-1} to −5.60 m a^{-1} for individual glaciers) for the nine land-terminating glaciers. This represents a 34% reduction in flow rates below the median altitude of land-terminating glaciers. In specific areas glacier velocity change of more than −10 m a^{-1} was detected, the location of which varied between glaciers (Figs. 2 and 3).

Five of the nine lake-terminating glaciers (all shown in Fig. 4) showed increased surface velocities over their lower reaches over the study period. Mean, ablation zone velocity change was 2.67 m a^{-1}, ranging from 0.18 m a^{-1} to 8.04 m a^{-1} for individual glaciers, but all five of these glaciers showed more substantial (10 m a^{-1} or more) acceleration towards their termini. These changes represent a 24% acceleration in flow rates below the median altitude of these five lake terminating glaciers.

The other four lake-terminating glaciers (shown in Fig. 5) decelerated over their ablation zones over the study period. Mean, ablation zone wide velocity change was −3.92 m a^{-1} (ranging from −0.36 m a^{-1} to −8.68 m a^{-1} for individual glaciers) for these four glaciers, a 34% reduction in flow rates below the median altitude. Again, maximum velocity change reached −10 m a^{-1} or more on three of these glaciers (Fig. 5).

Flow acceleration and deceleration caused opposing strain rates over the lower reaches of lake-terminating glaciers. Longitudinal strain rates $\left(\frac{dv}{dx}\right)$, averaged over the lowermost one kilometre of each glacier, using the 2013–2015 velocity dataset (Table 1), were positive (ranging from 0.03 to 0.06 a^{-1}), and flow was therefore extensional, over the five glaciers that accelerated over the study period. Strain rates were negative (ranging from −0.01 to −0.05 a^{-1}), and thus flow was compressional, over the terminal zone of the four glaciers that decelerated over the study period.

4.3. Lake-terminating glacier ice front position and lake expansion

All but one of the lake-terminating glaciers showed substantial cumulative ice front retreat between 1989 and 2015, ranging from 460 m to 1420 m (Fig. 6). Drogpa Nagtsang showed the largest ice front retreat (Fig. S2) despite the relatively recent formation of the lake (late 1980s). Some lake-terminating glaciers (Longmojian, Yanong North, Duiya) showed steady retreat rates, some (Trakarding, Yanong) showed a reduction in retreat rate, and some (Lhotse Shar, Kada, Drogpa Nagtsang)

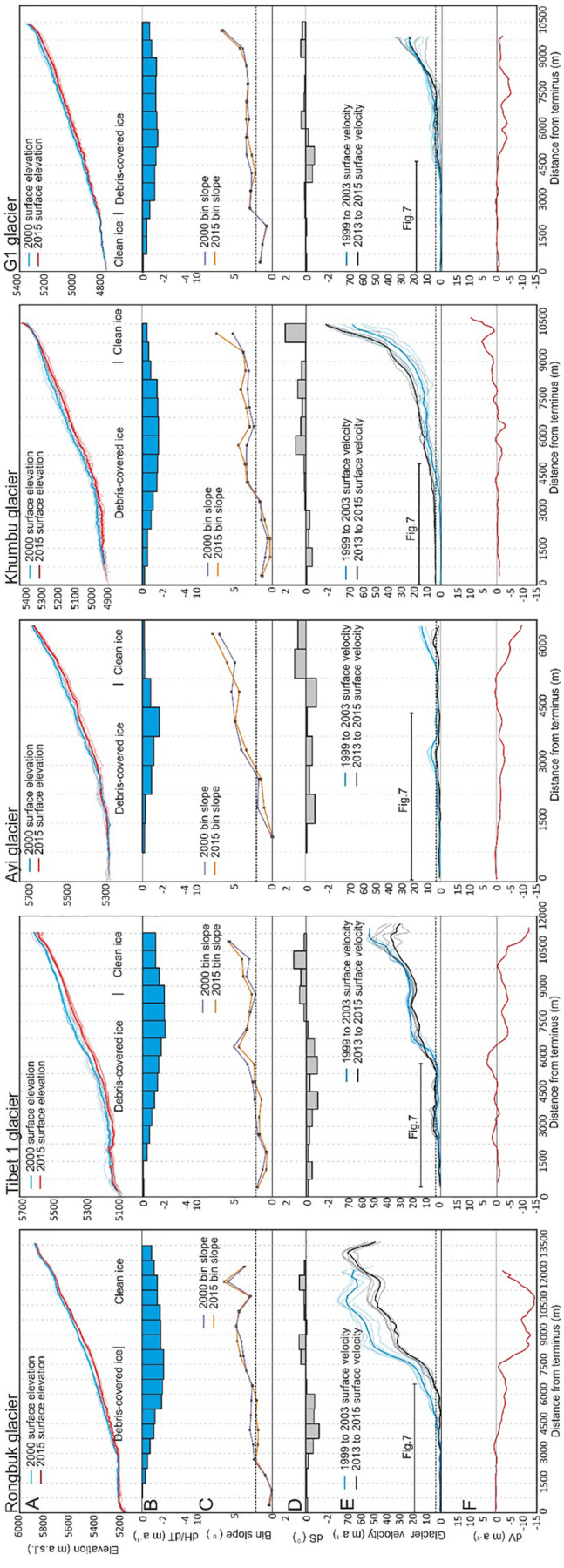

Fig. 2. Surface elevation (A), surface elevation change (dH/dT) (B), surface slope (C), surface slope change (dS) (D), surface velocity (E) and surface velocity change (dV) (F) of five land-terminating glaciers in the study area. The coverage of high-resolution satellite imagery shown in Fig. 7 is marked on velocity difference panels. Thresholds of surface slope (2°) and surface velocity (4 m a^{-1}) required for surface meltwater ponding are also marked.

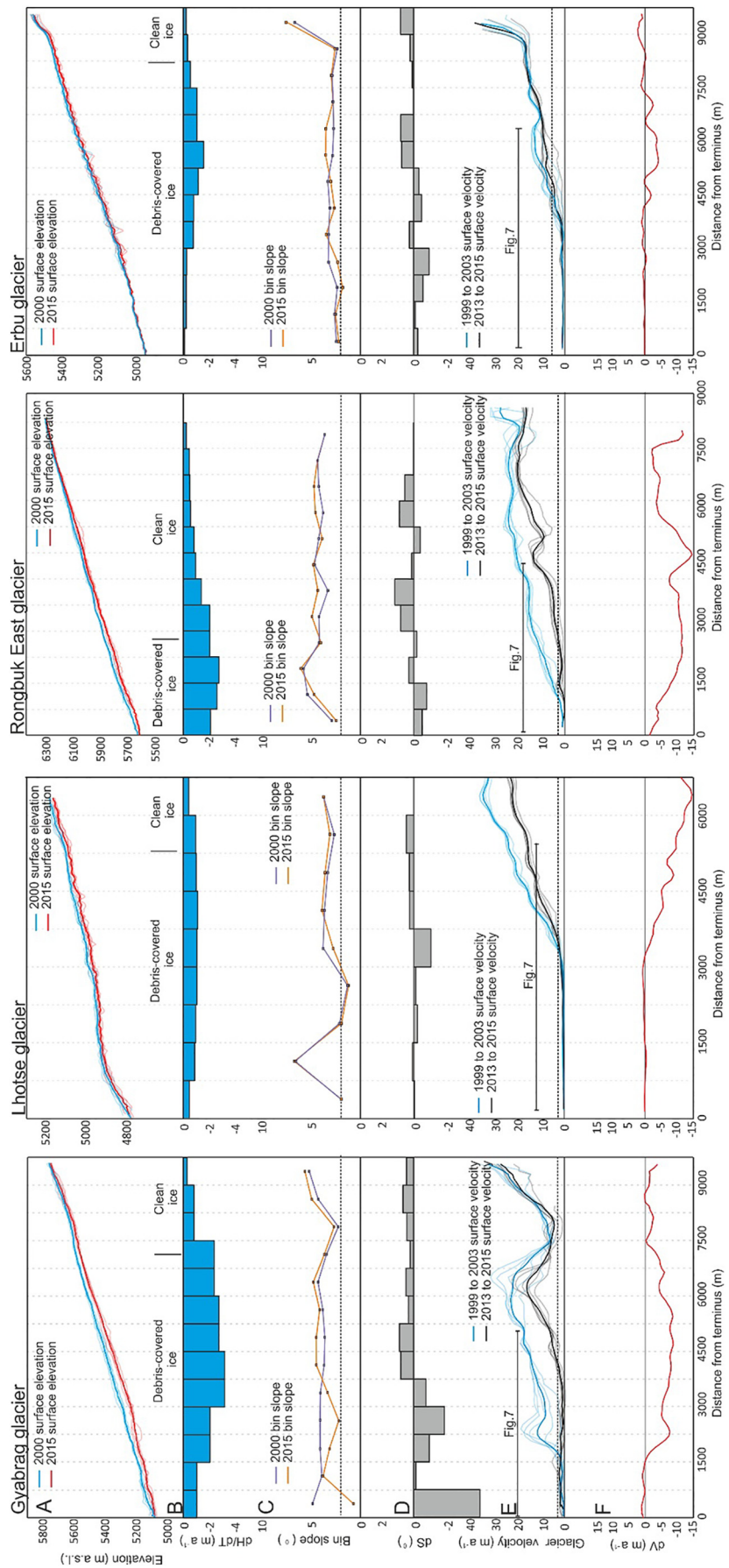

Fig. 3. Surface elevation (A), surface elevation change (dH/dT) (B), surface slope (C), surface slope change (dS) (D), surface velocity (E) and surface velocity change (dV) (F) of four land-terminating glaciers in the study area. The coverage of high-resolution satellite imagery shown in Fig. 7 is marked on velocity difference panels. Thresholds of surface slope (2°) and surface velocity (4 m a^{-1}) required for surface meltwater ponding are also marked.

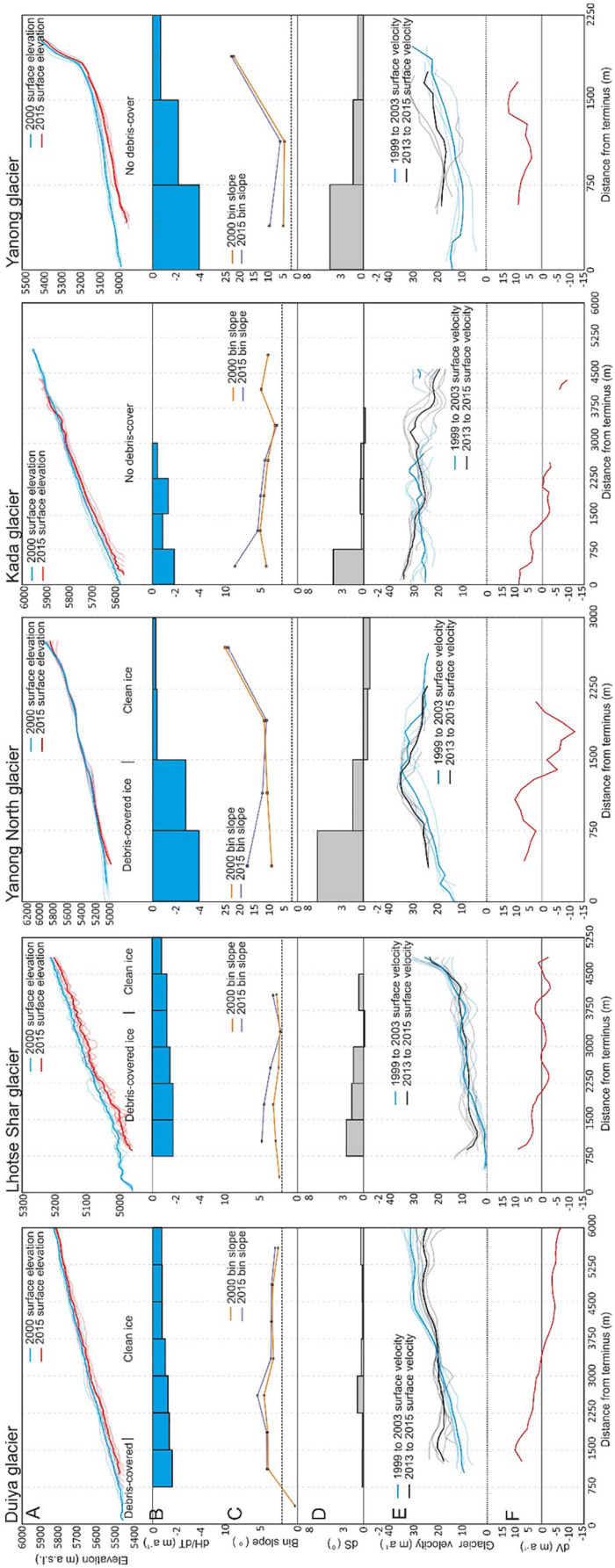

Fig. 4. Surface elevation (A), surface elevation change (dH/dT) (B), surface slope (C), surface slope change (dS) (D), surface velocity (E) and surface velocity change (dV) (F) of five lake-terminating glaciers in the study area. The coverage of high-resolution satellite imagery shown in Fig. 7 is marked on velocity difference panels. Thresholds of surface slope (2°) and surface velocity (4 m a^{-1}) required for surface meltwater ponding are also marked.

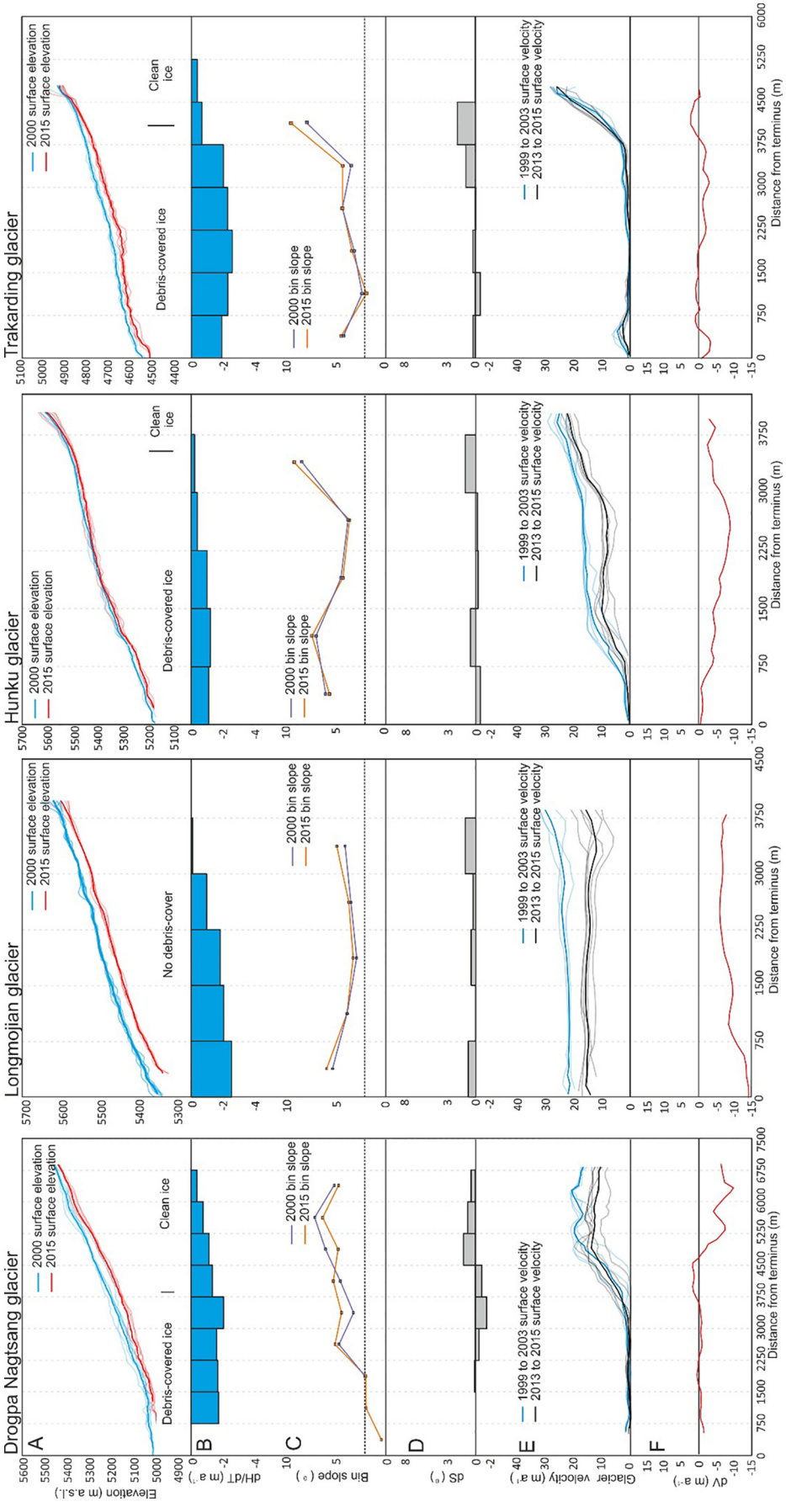

Fig. 5. Surface elevation (A), surface elevation change (dH/dT) (B), surface slope (C), surface slope change (dS) (D), surface velocity (E) and surface velocity change (dV) (F) of four lake-terminating glaciers in the study area. The coverage of high-resolution satellite imagery shown in Fig. 7 is marked on velocity difference panels. Thresholds of surface slope (2°) and surface velocity (4 m a^{-1}) required for surface meltwater ponding are also marked.

Table 1
Mean ablation zone velocity change, ice front position change, glacier geometry (surface slope) and terminal zone strain rate for lake-terminating glaciers. Terminal strain estimates are a mean value taken over the lowermost one kilometre of each glacier. Italicised values and glaciers are shown in Fig. 5, whereas plain text values and glaciers are shown in Fig. 4.

Glacier	Ablation zone velocity change ($m\,a^{-1}$)	Mean ice front position change rate 1989–2015 ($m\,a^{-1}$)	Mean change in slope (degrees)	Terminal strain rate (a^{-1})	Ice front width change (m)
Drogpa Nagtsang	*−1.96*	*−64.07*[a]	*0.04*	*−0.01*	*−14*
Longmojian	*−8.68*	*−13.98*	*0.41*	*−0.05*	*70*
Hunku	*−4.64*	*6.87*	*0.10*	*−0.01*	*−7*
Trakarding	*−0.40*	*−21.34*	*0.43*	*−0.01*	*−93*
Mean	*−3.92*	*−23.13*	*0.25*	*−0.02*	*−11*
Duiya	0.18	−33.62	0.33	0.06	−54
Yanong North	2.87	−21.99	2.13	0.06	31
Lhotse Shar	0.63	−30.19	0.95	0.03	227
Kada	1.63	−29.92	1.10	0.05	29
Yanong	8.04	−46.40	2.35	0.06	−68
Mean	2.67	−32.42	1.37	0.05	33

[a] Drogpa Nagtsang ice front position rates measured from 1996 to 2015.

showed an increase in retreat rate. Mean retreat rates ranged between $-14 \pm 3\,m\,a^{-1}$ (Longmojian) to $-64 \pm 5\,m\,a^{-1}$ (Drogpa Nagtsang) over the study period. Hunku Glacier is unique in having sustained a consistent ice front position between 1989 and 2015 (Fig. 6a).

Glacial lake area ranged from $0.24 \pm 0.06\,km^2$ (Hunku Glacier lake) to $1.47 \pm 0.19\,km^2$ (Tsho Rolpa, hosted by Trakarding Glacier) in 1989, and from $0.31 \pm 0.06\,km^2$ (Hunku Glacier lake) to $1.72 \pm 0.17\,km^2$ (Drogpa Nagtsang Glacier lake) in 2015. Glacial lake expansion rates again varied between glaciers, with some lakes (hosted by Drogpa Nagtsang, Lhotse Shar, Duiya and Yanong glaciers) expanding at increasing rates, some lakes (hosted by Hunku, Longmojian, Kada and Yanong glaciers) expanding at a steady rate, and one lake, hosted by Trakarding glacier, expanding at a diminishing rate (Fig. 6d).

The change in ice front widths that occurred alongside ice front retreat was highly variable over the study period (Table 1). The ice front width of five of the nine lake-terminating glaciers (Duiya, Yanong, Drogpa Nagtsang, Trakarding and Hunku glaciers) reduced by between −7 to −93 m over the study period. Ice front widening ranged from 29 to 227 m on the other four (Lhotse Shar, Kada, Yanong North and Longmojian) lake-terminating glaciers.

5. Discussion

There are clear differences in the evolving geometry and velocity of land- and lake-terminating glaciers in the Everest region. These contrasts suggest that very different processes have been operating on these glaciers of different terminus type throughout the study period.

5.1. Land-terminating glacier dynamics

The changes in the velocity and geometry of the land-terminating glaciers we have assessed were remarkably consistent, with all nine land-terminating glaciers experiencing similar surface geometry and velocity adjustments over the study period (Figs. 2 and 3). The reduced surface velocities we measured over the lower reaches of land-terminating glaciers (Figs. 2 and 3) suggests a longitudinally compressional flow regime exists here, which would have resulted in positive vertical ice motion and therefore surface elevation increases up-glacier of stagnant ice (Rounce et al., 2018). However, the highest thinning rates we measured occurred in such areas proximal to stagnant ice where

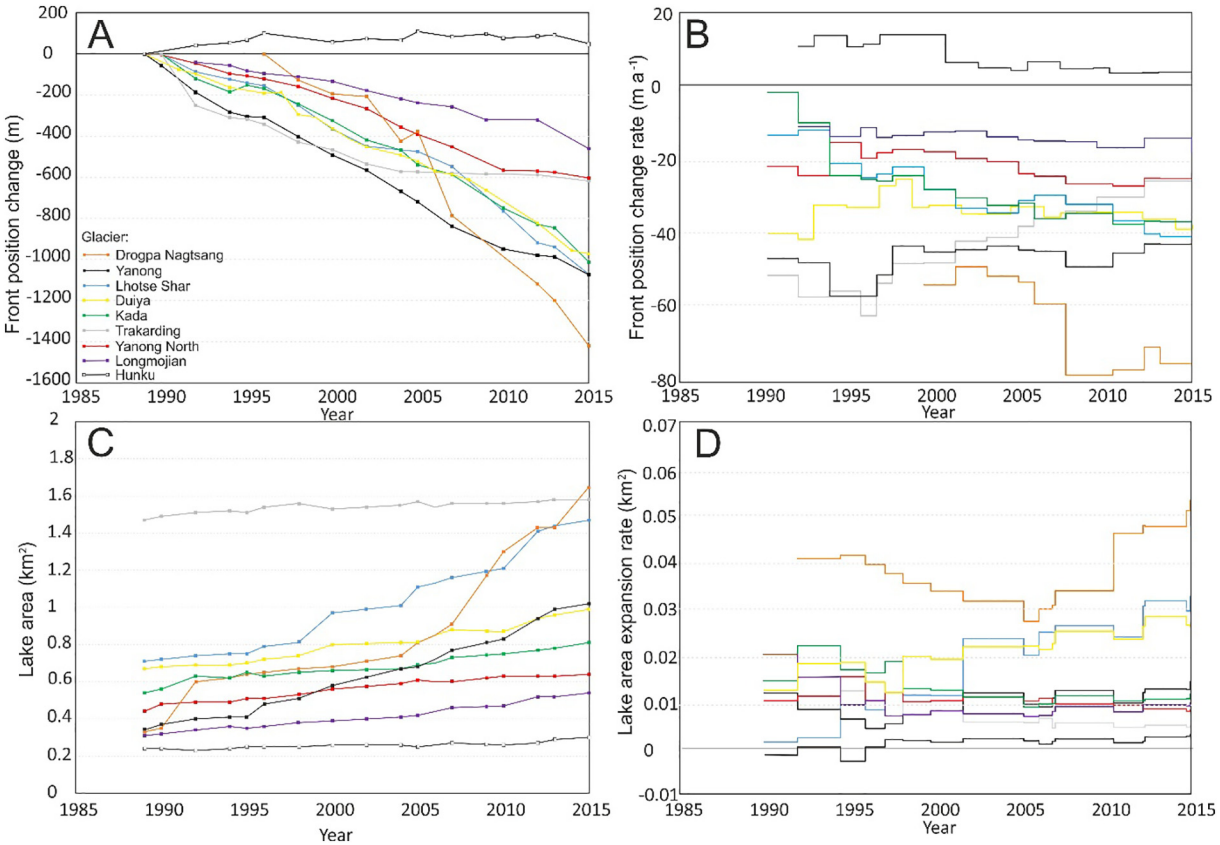

Fig. 6. A) Cumulative ice front; B) Ice front retreat rate; C) Lake area increase; and D) Lake area expansion rates for the 9 glaciers hosting lakes over the period 1989–2015.

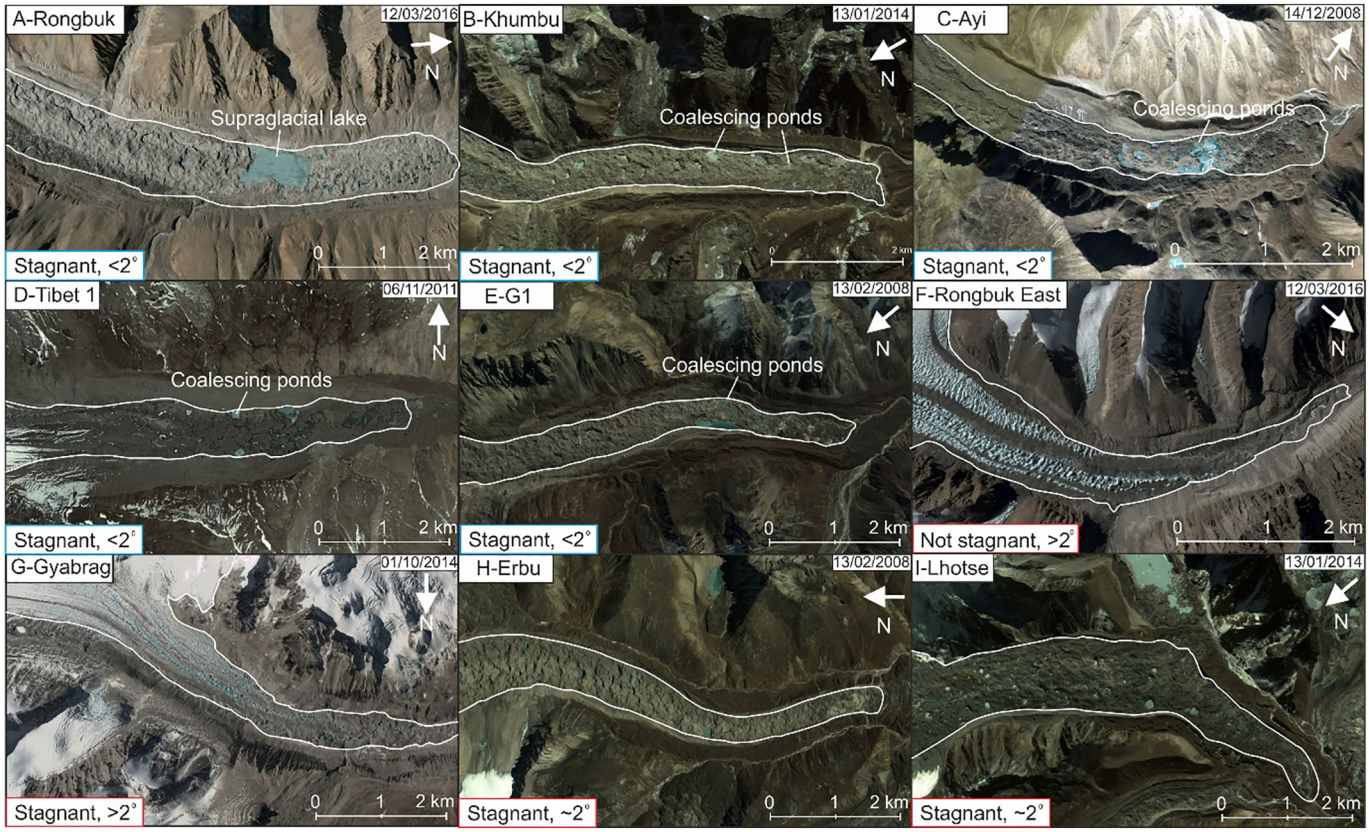

Fig. 7. Satellite imagery (Geoeye, Worldview) of the terminal areas of land-terminating glaciers we focus on in this study. Panels A-E are of glaciers that meet the criteria required for glacial lake formation, whereas panels F-I show glaciers that do not meet these criteria.

surface velocities declined (Figs. 2 and 3). Areas of the most substantial velocity reductions were coincident with the clean ice- debris covered transition zone of each land-terminating glacier, where debris thicknesses are commonly only a few centimetres (Nakawo et al., 1986; Rounce et al., 2018). Under such a thin debris layer, melt rates can be elevated above that of debris-free ice (Østrem, 1959; Nicholson and Benn, 2006; Evatt et al., 2015), and appear to have been of a sufficient magnitude to counter the vertical component of ice flux divergence and resulted in substantial surface lowering. The slight increases in surface gradient we have documented across the clean ice- debris covered boundary on each glacier (Figs. 2 and 3) have therefore occurred because surface lowering rates are elevated above that of clean ice in this zone of thin debris. Closer to glacier termini, the impact of both sub-debris melt and ice flux divergence is less substantial (Rounce et al., 2018) as debris thickness increases and ice flow is negligible, but surface lowering and surface gradient reductions still occurred (Figs. 2 and 3). This is presumably because of the impact of much expanded supraglacial pond and ice cliff networks on land-terminating glaciers in the area (Watson et al., 2016, 2017), which act as hot-spots of melt on debris covered glaciers.

The reduction of surface gradients (Figs. 2 and 3) and prolonged ice thinning on glaciers in the Everest region (cf. Bolch et al., 2011) will have led to a reduction in driving stress (Cuffey and Paterson, 2010; Benn et al., 2012) and therefore glacier velocities, not just over our study period, but also during preceding decades. Figs. 2 and 3 show that this process has clearly been in operation on the lower reaches of land-terminating glaciers in the Everest region; large areas display little or no flow up to several kilometres from their termini, surface gradients are low across these stagnant areas (Figs. 2 and 3)., and the greatest differences in surface velocity were seen on glaciers (Gyabrag and Rongbuk) with the greatest percentage decrease in surface gradient (Figs. 2 and 3). Thakuri et al. (2014) show a 17.1 ± 3.1% increase in the total area of debris covered ice in the Everest Region since the 1960's, which has predominantly occurred as an up-glacier migration of the debris covered-clean ice transition zone. The debris mantle on this part of a debris covered glacier is thin (Rounce and McKinney, 2014), thus surface lowering is amplified and the longitudinal surface gradient has reduced (Figs. 2 and 3). Continued expansion of the debris cover up-glacier could therefore also cause areas of reducing surface slope to spread, with consequent further reductions in ice flow.

An additional process that may be contributing to glacier deceleration is a reduction in accumulation and therefore a reduction in ice flux to lower elevations (e.g. Benn et al., 2012; Nuimura et al., 2011; Heid and Kääb, 2012). Increased snow line altitudes (Thakuri et al., 2014), decreasing precipitation (Salerno et al., 2015) and reduced accumulation between 1970 and 2001 detected in an ice core on the northern side of the orographic divide in the Everest region (Kaspari et al., 2008) could all be taken as evidence of reduced accumulation over our study period. However, a change in accumulation would only immediately impact on the upper reaches of each glacier, and would take time to propagate down to the ablation zone, where we have documented the most substantial changes in glacier velocity and geometry. Knowledge of the response time of Himalayan glaciers to perturbations in accumulation is currently relatively limited. Scherler et al. (2011) estimated the response time of 286 glaciers across the Himalaya, some of which were debris covered and some of which were devoid of debris cover. Scherler et al. (2011) found that the neither the response time nor the climate sensitivity of debris covered glaciers could be estimated using the same attributes as clean ice glaciers (e.g. Leclercq and Oerlemans, 2012), and suggest that the impact of an insulating debris layer on terminus retreat rates precludes their use as indicators of recent climate change. Banerjee and Shankar (2013) suggested that debris covered glaciers may exhibit a > 100 year 'stationary period' in response to a warming climate and associated ELA increase, with little to

no terminus retreat occurring during this period. Of the nine land-terminating glaciers shown in Figs. 2 and 3, eight are stationary over their lower reaches, and have been since at least the date of our first velocity observations (1999). Thakuri et al. (2014) also documented little ($-6.1 \pm 0.2\,m\,a^{-1}$) ice front retreat over land-terminating glacier in the Everest region over the period 1962 to 2011. However, without more temporally extensive observations of glaciers length variations and glacier velocity, it is difficult to suggest how long these glaciers may have been in the stationary state suggested by Banerjee and Shankar (2013), and how close they may be to a different mode of response to continued warming.

5.2. Lake-terminating glacier dynamics

The velocity and geometry change data we have generated for lake-terminating glaciers can be separated into two distinct groups (Figs. 4 and 5). The increased velocity of the five lake-terminating glaciers shown in Fig. 4, and the associated expansion of the glacial lakes they host (Fig. 6), suggests a link between lake expansion and glacier behaviour in these 5 cases. Conversely, the flow velocity deceleration of the four lake-terminating glaciers shown in Fig. 5 suggests glacial lake expansion may not have significantly impacted their dynamics over the study period. These observations suggest two contrasting sets of processes have been in operation on lake-terminating glaciers in the Everest region over the last 15 years.

The two main components of frontal ablation on marine- and lake-terminating glaciers are mechanical calving and the subaqueous melt of the ice front in contact with water (Carrivick and Tweed, 2013). Either of these melt components can be the dominant factor in ice front position retreat across different water terminating glaciers in both space and time (Truffer and Motyka, 2016). The magnitude of subaqueous melt depends primarily on the temperature of the proglacial water body and its salinity. Small, proglacial lakes are typically much cooler than water in a coastal, marine setting (Chikita, 2007; Truffer and Motyka, 2016), and there is little density contrast between glacial meltwater and the freshwater of the proglacial water body to drive the circulation of water and enhance subaqueous melt. Indeed, Trüssel et al. (2013) found that on one Alaskan, lake-terminating glacier (Yakutat Glacier), the observed thinning could be entirely explained by surface melt, and that there was no contribution from subaqueous melt. Data on the temperature and structure of the proglacial lakes in our study area are limited. Chikita (2007) show a water temperature of 2–3 °C for much of the water column in Imja Tsho and Tsho Rolpa with only a shallow (~20 m of a total water depth of 120 m or more for both lakes) layer of warmer water (3–6 °C) towards the surface of the lake. These temperatures are similar to those of the lake at the front of Yakutat Glacier (water temperatures of between 0.5 and 1.5 °C– Trüssel et al., 2013), and we therefore suggest that such conditions cannot reasonably account for the mass loss rates that have been detected on these glaciers (King et al., 2017). It is likely that the warm surface layer documented by Chikita (2007) and wind driven water currents (Sakai et al., 2009) would drive the development of a thermal notch as has been documented on other lake-terminating glaciers (Warren and Kirkbride, 2003; Trüssel et al., 2013), but only over a limited vertical extent. We therefore focus the following discussion of lake-terminating glacier retreat on the impact of mechanical calving on these glaciers.

The acceleration of the five lake-terminating glaciers shown in Fig. 4, and their sustained or accelerating ice front retreat rates (Fig. 6), suggests a link between lake development and glacier behaviour in these 5 cases over the last 15 years. Benn et al. (2007) outline three models of water-terminating glacier behaviour, the third of which, which considers both lateral and basal drag as the dominant resisting stress to ice flow, is most appropriate for the topographically constrained glaciers we have assessed in this study. The model of Benn et al. (2007) is applicable to glaciers that have developed a lake of sufficient depth to interact with the glacier at its bed. In this model, dynamic water-terminating glacier retreat is triggered by an imposed thinning (an increase in surface melt, for example) that alters the level of effective pressure- the difference between ice overburden pressure and water pressure. Decreasing effective pressure causes ice flow acceleration and a positive feedback ensues between acceleration, increased longitudinal strain, dynamic thinning and calving retreat. Calving retreat becomes dominant because extensional flow causes the deepening of crevasses in the terminal zone of each glacier, and because thinning reduces the freeboard level (the height of the glacier surface above lake level), increasing the likelihood that crevasses will reach the waterline. The strength of this feedback differs depending on the magnitude of resisting stresses (lateral and basal drag), particularly where the glacier is grounded, with the maximum attainable glacier velocity being lower where resisting stresses are high, and vice versa. The magnitude of the feedback between these processes can also be moderated by surface gradient (Benn et al., 2007).

We have documented the occurrence of a number of the processes that combine to set up the positive feedback proposed by Benn et al. (2007) to drive increased ice loss on lake-terminating glaciers. The five lake-terminating glaciers shown in Fig. 4 have experienced substantial terminal zone thinning (shown here and in Bolch et al., 2011; Nuimura et al., 2012), flow acceleration (Fig. 4) and increased longitudinal strain (Table 1), and sustained or accelerating ice front retreat rates over the last 26 years (Fig. 6). We therefore suggest that the set of processes incorporated into the model of Benn et al. (2007) are in operation on some Himalayan lake-terminating glaciers, as has been inferred on lake-terminating glaciers in other glacierised regions (Muto and Furaya, 2013; Robertson et al., 2013; Sakakibara and Sugiyama, 2014; Chernos et al., 2016). The variability in cumulative glacier front retreat and glacier front retreat rates we show in Fig. 6, and the broad range of mass balance estimates generated for lake-terminating glaciers by King et al. (2017), likely reflects the variable response of glaciers depending on their topographic setting (i.e. valley morphology), width and surface slope- all factors that influence levels of basal and lateral drag (Pementel et al., 2010; Adhikari and Marshall, 2012).

The slowdown of the four lake-terminating glaciers shown in Fig. 5 suggests glacial lake expansion may not have been the dominant factor in their evolving dynamics over our study period, despite the physical link between each lake and its host glacier. Three of these four glaciers (Trakarding, Hunku and Longmojian) have hosted glacial lakes since at least the 1970's (Sakai et al., 2000; Bajracharya et al., 2007), and may have been thinning, like other glaciers in the Everest region (Bolch et al., 2011), over a similar timescale, including our study period (King et al., 2017). The deceleration of these three glaciers may therefore be a result of a reduction in driving stress and increased resistive stresses (lateral and basal drag) as the terminal zone of these glaciers narrowed (Table 1) in association with thinning (Pementel et al., 2010; Adhikari and Marshall, 2012). Reduced ice flow, combined with increased resistive stresses, would have reduced levels of longitudinal stretching, transverse crevassing and therefore calving, when compared with formerly elevated surface velocities (Benn et al., 2012). The diminishing ice front retreat rate of Trakarding Glacier may be evidence of this process. The less substantial terminus proximal surface lowering on Trakarding and Hunku glaciers over the study period likely indicates that surface melt is now the dominant ice loss process, rather than calving and dynamic ice front retreat.

The behaviour of Drogpa Nagtsang cannot be explained by these same processes given the relatively recent formation of its lake (Fig. 6). In this case, the lake that has developed may still be supraglacial, and is therefore too shallow (or the glacier still too thick) to initiate more dynamic glacier behaviour. Until this glacier thins, or the lake melts through the remaining glacier ice, flow acceleration through an adjustment of effective pressure will not occur. The changes in glacier velocity and geometry we have observed for this glacier (Fig. 5) are more akin to those of a land-terminating glacier, as would be the case on other glaciers that have recently developed lakes that are yet to influence their dynamics.

5.3. Preconditioning of glacier surfaces for lake development- can lake formation be predicted?

Previous studies have suggested that under particular geometric and dynamic conditions surface melt ponds are likely to coalesce, enabling glacial lakes to form. Quincey et al. (2007) and Reynolds et al. (2000) suggested that meltwater ponding and coalescence is most likely to occur where glacier surfaces are of < 2° slope and effectively 'stagnant'. If a glacier surface is steeper than this threshold or flowing actively, meltwater will continue to drain down-glacier, or crevasse formation (from active flow) will provide pathways for englacial meltwater re-routing, most likely towards the edge of a glacier, where lateral drag causes enhanced strain and ice surface fracturing (Cuffey and Paterson, 2010). Using the criteria of Quincey et al. (2007) and Reynolds et al. (2000) we are able to assess whether any of the land-terminating glaciers we have examined are primed for glacial lake development.

Fig. 7 shows the terminal regions of the nine land-terminating glaciers depicted in Figs. 2 and 3. Of these glaciers, five (those in Fig. 2) show substantial supraglacial pond formation (water bodies of < 20,000 m^2 area), or, in the case of Rongbuk Glacier, supraglacial lake formation (Watson et al., 2016). These glaciers showed large areas of < 2° slope and negligible ice flow in the first epoch of our DEM and velocity time series, and an expanded area of the same conditions at the end of our study period. Watson et al. (2016) documented substantial increases in the ponded area of some of these glaciers over our study period, as did Chen et al. (2014) for the supraglacial lake on Rongbuk Glacier, so it is likely that these glaciers are already in the early stages of glacial lake development. Continued sub-debris melt in the middle reaches of these glaciers would further decrease the surface gradient and provide meltwater, both aiding supraglacial pond and lake expansion.

Four of the nine land-terminating glaciers we studied (shown in Fig. 3) fail to meet one or both of the criteria proposed by Quincey et al. (2007) and Reynolds et al. (2000) (Fig. 7), and have not experienced pond coalescence. Gyabrag Glacier (Fig. 7 panel G) showed surface gradient values greater than the 2° threshold (mean of 4.03°) required for effective meltwater ponding. Rongbuk East (Fig. 7 panel F) showed substantial ice flow to its terminus (Fig. 3c), as well as being too steep (mean 4.15°) for water to collect. Small areas of Lhotse and Erbu glaciers meet the velocity and surface gradient thresholds (Figs. 3b & d), and some ponding is evident on these glaciers (Fig. 7, panels H & I). Lhotse and Erbu glaciers may therefore be in the early stages of pond coalescence, and further surface lowering will aid water ponding here. Collectively, these observations suggest the criteria outlined by Quincey et al. (2007) and Reynolds et al. (2000) are appropriate as a first-pass method to identify glaciers that may or may not be susceptible to glacial lake formation.

5.4. Implications of lake-terminating glacier retreat

We have shown here how different ice mass loss processes may drive the evolution of lake and land-terminating glaciers in the Himalaya. Lake-terminating glaciers experience different phases of retreat and ice loss as the lake they host expands. Initially, a phase of lake expansion may occur that is not accompanied by amplified glacier mass loss. As the lake level rise or the host glacier thins, calving can occur, front retreat rates may accelerate, the glacier surface profile steepens, and ice flow rates increase. Towards the later stages of lake growth, after a sustained period of ice front retreat and glacier thinning, which reduce driving stresses and increase resisting stresses (lateral and basal drag) due to glacier narrowing (e.g. Adhikari and Marshall, 2012), lake-terminating glaciers slowdown and their retreat rate diminishes. As the total number of glacial lakes seems to be increasing, not just in the Everest Region, but across the Himalaya (Zhang et al., 2015; Nie et al., 2017), it can be inferred that glacial lake expansion will serve to amplify the future mass loss of their host glaciers. Similar observations of amplified ice loss from lake terminating glaciers have been made elsewhere in the Himalaya. For example, Basnet et al. (2013) examined the area loss of 38 glaciers in the Sikkim Himalaya, India, from 1990 to 2014, and found that the total area loss of the 23 lake-terminating glaciers in their sample was five times greater than the total area loss of land terminating glaciers. Wang et al. (2017) observed similarly amplified retreat rates of lake terminating glaciers (six times higher) when compared with land terminating glaciers in the Hengduan Shan region of the southeastern Tibetan Plateau from 1990 to 2014.

It is unclear how long it takes for lake growth to initiate more dynamic glacier behaviour. The development of the large (1.38 km^2) supraglacial lake on Drogpa Nagtsang Glacier has been rapid (Fig. 6), but there is no evidence for a resulting effect on the glacier velocity or geometry. Similarly, Rongbuk Glacier has developed a large (0.48 km^2) supraglacial lake since the early 1990s (Chen et al., 2014), but the glacier is stagnant over the area the lake occupies, and the gradient of its lower reaches has reduced as the lake has persisted. Without detailed ice thickness and multi-temporal lake bathymetry datasets, which are both sparse in the Everest region and across the Himalaya as a whole, predictions of when supraglacial lake growth may impact ice dynamics are obviously difficult to make, and may be glacier specific, depending on deepening rates of individual lakes.

Once a full-depth lake has developed and has begun to impact on glacier velocities and thinning rates, the duration of amplified ice mass loss will depend on the spatial extent of enhanced thinning and the magnitude of acceleration. This study has shown that substantial glacier length reductions could occur over a few decades. Although the front retreat rates we show (Fig. 6) may seem moderate, the cumulative total front retreat on the nine lake-terminating glaciers in our sample accounted for an average glacier length reduction of almost 20% (ranging from 11 to 41%) over 25 years. Throughout this period of ice front retreat, surface lowering rates over the terminal regions of lake-terminating glaciers may be more than double those of neighbouring land-terminating glaciers (King et al., 2017), and this impacts on the mass balance of each lake-terminating glacier (Bolch et al., 2011; King et al., 2017). The scale of ice loss is also likely to be large on Himalayan glaciers that have especially low surface gradients, as the presence of a glacial lake pins the glacier terminus to a certain altitude and precludes the stabilising feedback of the glacier retreating to a higher altitude (Truffer and Motyka, 2016). Glaciers with long ablation zones of a similar altitude, such as those shown in Fig. 2, will therefore have to retreat substantially up-valley before they can separate vertically from their glacial lake.

The expansion of a glacial lake heightens GLOF hazard directly because; 1) glacial lake expansion increases the area into which mass movements (from both the host glacier and surrounding terrain) can enter and form an overtopping wave, and 2) an increase in lake volume increases lake depth and hence the water burden pressure on the terminal moraine dam. An increase in the calving flux or frequency of large calving events may also lead to more frequent wave or overtopping events (Fujita et al., 2013; Westoby et al., 2014). Gardelle et al. (2011) documented a 20% increase in the area of glacial lakes in the Everest region over the period 2000–2009, and our ice front position data shows that this trend has continued through to 2015. Rounce et al. (2017) modelled potential lake expansion and mass-movement trajectories in the Everest region and showed that Imja Tsho could become more hazardous as the lake becomes more proximal to avalanche prone terrain up-valley. The same scenario can be envisaged for other glacial lakes, particularly those that have formed on glaciers fed by steep headwalls and whose primary source of accumulation if from avalanches, as is common in the Himalaya (Benn et al., 2001; Itturizaga, 2011).

5.5. Outlook

A number of recent modelling studies (e.g. Rowan et al., 2015; Shea

et al., 2015; Anderson and Anderson, 2016) have successfully replicated the changes in geometry and velocity of Himalayan land-terminating glaciers in a state of negative mass balance that we describe above. However, the complete contrast in the evolution of lake-terminating glaciers demands a modified approach be taken to simulate their behaviour under different climate scenarios. The similarity of the velocity and thinning regimes predicted by the modelling work of studies such as Benn et al. (2007) with the data we present here suggests that many elements of lake-terminating glacier behaviour in the Himalaya can be predicted. The calculation of the time taken for a full depth lake to form and the accommodation space available for a glacial lake is currently limited by a paucity of well-constrained glacier bed topography and ice thickness data, both of which may be suitable foci for future work in the region. Where a glacier is already hosting a glacial lake, measurements of lake bathymetry (e.g. Yamada, 1998; Somos-Valenzuela et al., 2014) are important as, alongside the down-glacier velocity gradient, the difference between ice thickness and water depth is considered a primary control on lake-terminating glacier terminus position (Benn et al., 2007). Detailed measurements of glacial lake depth are currently only available for Imja Tsho in our study area. Comparison of the bathymetric surveys presented by Chikita (2007), Fujita et al. (2009) and Somos-Valenzuela et al. (2014) suggests up to 30 m of deepening in this lake between 1996/1997 and 2012, which may have been a large contributing factor in the dynamic changes of its host glacier (Lhotse Shar Glacier) that we have shown.

6. Conclusions

Analysis of a time series of DEMs and glacier surface velocity data has revealed contrasting geometric and dynamic evolution of lake- and land-terminating glaciers in the Everest region of the Central Himalaya over the last 15 years. Land-terminating glaciers showed similar thinning patterns, changes in surface gradient and changes in velocity. These glaciers thinned most close to the debris-clean ice transition zone, became shallower over their lower reaches and decelerated over the study period. Lake-terminating glacier behaviour can be characterised by two distinct groups. Five of the nine lake-terminating glaciers we assessed showed increased surface velocities alongside enhanced terminal thinning and increased surface gradients. These five glaciers show steady or increasing ice front retreat rates. The remaining four lake-terminating glaciers showed low magnitude glacier surface steepening, reduced glacier surface velocities and steady or diminishing ice front retreat rates. We suggest that this contrasting lake-terminating glacier behaviour represents two different phases of glacier-lake interaction; one where a dynamic link exists between lake expansion and glacier mass loss, with a positive feedback operating between decreasing effective pressure, increased ice velocities, enhanced thinning and longitudinal strain, enhancing mass loss. The other is representative of either an early phase of lake development, during which a glacial lake does not substantially impact on its host glaciers dynamics, or a late stage where a glacier begins to disconnect from the lake it hosts. During either of these stages, changes in glacier velocity or geometry will be more akin to those of a land-terminating glacier.

The timeline of lake development and coincident glacier retreat remains uncertain, but we have documented substantial ice front retreat over a few decades in the Everest region of the central Himalaya. An improved understanding of the bed topography and ice thickness of glaciers primed for lake development would undoubtedly aid efforts to model future lake-terminating glacier behaviour. In their absence, glacier geometry and glacier velocity data can at least be used as a first-pass tool to identify glaciers that are preconditioned for lake development. These data may serve as early warning for those living and working in the region who may need to adapt to an increasing hazard over coming decades, but additionally, they may also be used by numerical modellers aiming to simulate glacier evolution under varying climatic scenarios, as the need to consider glacier-lake interactions becomes increasingly pertinent.

Supplementary data to this article can be found online at https://doi.org/10.1016/j.gloplacha.2018.05.006.

Acknowledgements

OK is a recipient of a NERC SPHERES DTP PhD Studentship (grant award NE/L002574/1). AD was supported by funding from the NASA Cryosphere Program. The research was conducted at the Jet Propulsion Laboratory, California Institute of Technology under contract with the National Aeronautics and Space Agency.

Supplementary data

References

Adhikari, S., Marshall, S.J., 2012. Parameterization of lateral drag in flowline models of glacier dynamics. J. Glaciol. 58 (212), 1119–1132. http://dx.doi.org/10.3189/2012JoGG12J018.

Anderson, L.S., Anderson, R., 2016. Modeling debris-covered glaciers: response to steady debris deposition. Cryosphere 10, 1105–1124. http://dx.doi.org/10.5194/tc-10-1105-2016.

Bajracharya, S.R., Mool, P.K., Shrestha, B.R., 2007. Impact of Climate Change on Himalayan Glaciers and Glacial Lakes: Case Studies on GLOF and Associated Hazards in Nepal and Bhutan. International Centre for Integrated Mountain Development (ICIMOD), Kathmandu.

Bajracharya, Samjwal, Shrestha, Finu, Bajracharya, Samjwal, Maharjan, S.B., Guo, Wanqin, 2014. GLIMS Glacier Database. National Snow and Ice Data Center, Boulder, CO. http://dx.doi.org/10.7265/N5V98602.

Banerjee, A., Shankar, R., 2013. On the response of Himalayan glaciers to climate change. J. Glaciol. 59 (215), 480–490. http://dx.doi.org/10.3189/2013JoG12J130.

Basnet, S., Kulkarni, A.V., Bolch, T., 2013. The influence of debris cover and glacial lakes on the recession of glaciers in Sikkim Himalaya, India. J. Glaciol. 59 (218). http://dx.doi.org/10.3189/2013JoG12J184.

Benn, D.I., Wiseman, S., Hands, K.A., 2001. Growth and drainage of supraglacial lakes on debris-mantled Ngozumpa Glacier, Khumbu Himal, Nepal. J. Glaciol. 47 (159), 626–638. http://dx.doi.org/10.3189/172756501781831729.

Benn, D.I., Hulton, N.R.J., Mottram, R.H., 2007. 'Calving laws', 'sliding laws' and the stability of tidewater glaciers. Ann. Glaciol. 46. http://dx.doi.org/10.3189/172756407782871161.

Benn, D.I., Bolch, T., Hands, K., Gulley, J., Luckman, A., Nicholson, L.I., Quincey, D., Thompson, S., Toumi, R., Wiseman, S., 2012. Response of debris-covered glaciers in the Mount Everest region to recent warming, and implications for outburst flood hazards. Earth Sci. Rev. (114), 156–174. http://dx.doi.org/10.1016/j.earscirev.2012.03.008.

Bolch, T., Pieczonka, T., Benn, D.I., 2011. Multi-decadal mass loss of glaciers in the Everest area (Nepal Himalaya) derived from stereo imagery. Cryosphere (5), 349–358. http://dx.doi.org/10.5194/tc-5-349-2011.

Braithwaite, R.J., Raper, S.C.B., 2009. Estimating equilibrium-line altitude (ELA) from glacier inventory data. Ann. Glaciol. (50), 127–132. http://dx.doi.org/10.3189/172756410790595930.

Burgess, E., Forster, R.E., Larsen, C.F., 2013. Flow velocities of Alaskan glaciers. Nat. Commun. 4, 2146. http://dx.doi.org/10.1038/ncomms3146.

Carrivick, J.L., Tweed, F.S., 2013. Proglacial lakes: character, behaviour and geological importance. Quat. Sci. Rev. (78), 34–52. http://dx.doi.org/10.1016/j.quascirev.2013.07.028.

Carrivick, J.L., Tweed, F.S., 2016. A global assessment of the societal impacts of glacier outburst floods. Glob. Planet. Chang. (144), 1–16. http://dx.doi.org/10.1016/j.gloplacha.2016.07.001.

Chen, W., Doko, T., Liu, C., Ichinose, T., Fukui, H., Feng, Q., Gou, P., 2014. Changes in Rongbuk Lake and Imja lake in the Everest Region of Himalaya, The International Archives of the Photogrammetry, Remote Sensing and Spatial Information Sciences, Volume XL-2, ISPRS Technical Commission II Symposium. http://dx.doi.org/10.5194/isprsarchives-XL-2-259-2014.

Chernos, M., Koppes, M., Moore, R.D., 2016. Ablation from calving and surface melt at lake-terminating Bridge Glacier, British Columbia, 1984–2013. Cryosphere 10, 87–102. http://dx.doi.org/10.5194/tc-10-87-2016.

Chikita, K.A., 2007. Topographic effects on the thermal structure of Himalayan glacial lakes: observations and numerical simulation of wind. J. Asian Earth Sci. (30), 344–352. http://dx.doi.org/10.1016/jseas.2006.10.005.

Cuffey, K.H., Paterson, W.S.B., 2010. The Physics of Glaciers, 4th ed. Elsevier, Burlington.

Dehecq, A., Gourmelen, N., Trouve, E., 2015. Deriving large-scale glacier velocities from a complete satellite archive: application to the Pamir-Karakoram-Himalaya. Remote Sens. Environ. 162, 55–66. http://dx.doi.org/10.1016/j.rse.2015.01.031.

Evatt, G., Abrahams, I., Heil, M., Mayer, C., Kingslake, J., Mitchell, S., Fowler, A.C., Clark, C., 2015. Glacial melt under a porous debris layer. J. Glaciol. 61 (229), 825–836. http://dx.doi.org/10.3189/2015JoG14J235.

Fitch, A.J., Kadyrov, A., Christmas, W.J., Kitller, J., 2002. Orientation correlation. In: Proceedings of the British Machine Conference. BMVA Press pp.11.1–11.10. https://doi.org/10.5244/C.16.11.

Fujita, K., Sakai, A., Nuimura, T., Yamaguchi, S., Sharma, R.R., 2009. Recent changes in Imja Glacial Lake and its damming moraine in the Nepal Himalaya revealed by in situ

surveys and multi-temporal ASTER imagery. Environ. Res. Lett. (4), 1–7. http://dx.doi.org/10.1088/1748-9326/4/4/045205.
Fujita, K., Sakai, A., Takenaka, S., Nuimura, T., Surazakov, A.B., Sawagaki, T., Yamanokuchi, T., 2013. Potential flood volume of Himalayan glacial lakes. Nat. Hazards Earth Syst. Sci. 13 (7), 1827–1839. http://dx.doi.org/10.5194/nhess-13-1827-2013.
Gardelle, J., Arnaud, Y., Berthier, E., 2011. Contrasted evolution of glacial lakes along the Hindu Kush Himalaya mountain range between 1990 and 2009. Glob. Planet. Chang. (75), 47–55. http://dx.doi.org/10.1016/j.gloplacha.2010.10.003.
Heid, T., Kääb, A., 2012. Repeat optical satellite images reveal widespread and long term decrease in land-terminating glacier speeds. Cryosphere (6), 467–478. http://dx.doi.org/10.5194/tc-6-467-2012.
International Centre for Integrated Mountain Development (ICIMOD), 2011. Glacial Lakes and Glacial Lake Outburst Floods in Nepal. ICIMOD, Kathmandu, Nepal.
Itturizaga, L., 2011. Trends in 20th century and recent glaciers fluctuations in the Karakoram Mountains. Z. Geomorphol. (55), 205–231. http://dx.doi.org/10.1127/0372-8854/2011/0055S3-0059.
Kaspari, S., Hooke, R., Le, B., Mayewski, P.A., Kang, S.C., Hou, S.G., Qin, D.H., 2008. Snow accumulation rate on Qomolangma (Mount Everest), Himalaya: synchroneity with sites across the Tibetan Plateau on 50-100 year timescales. J. Glaciol. 54 (185), 343–352. http://dx.doi.org/10.3189/002214308784886126.
Kääb, A., Berthier, E., Nuth, C., Gardelle, J., Arnaud, Y., 2012. Contrasting patterns of early 21st century glacier mass change in the Himalayas. Nature 488, 495–498. http://dx.doi.org/10.1038/nature11324.
King, O., Quincey, D.J., Carrivick, J.L., Rowan, A.V., 2017. Spatial variability in mass loss of glaciers in the Everest region, central Himalayas, between 2000 and 2015. Cryosphere (11), 407–426. http://dx.doi.org/10.5194/tc-11-407-2017.
Leclercq, P.W., Oerlemans, 2012. Global and hemispheric temperature reconstruction from glacier length fluctuations. J. Clim Dyn 38. http://dx.doi.org/10.1007/s00382-011-1145-7.
McNabb, R.W., Hock, R., 2014. Alaska tidewater glacier terminus positions, 1948–2012. J. Geophys. Res. Earth Surf. (119), 153–167. http://dx.doi.org/10.1002/2013JF002915.
Melkonian, A., Willis, M.K., Pritchard, M.E., 2016. Stikine icefield mass loss between 2000 and 2013/2014. Front. Earth Sci. 4 (89). http://dx.doi.org/10.3389/feart.2016.0089.
Miles, E.S., Willis, I.C., Arnold, N.S., Steiner, J., Pellicciotti, F., 2016. Spatial, seasonal and interannual variability of supraglacial ponds in the Langtang Valley, 1999–2013. J. Glaciol. 63 (237), 88–105. http://dx.doi.org/10.1017/jog.2016.120.
Moon, T., Joughin, I., 2008. Changes in ice front position on Greenland's outlet glaciers from 1992 to 2007. J. Geophys. Res.(113), F02022. http://dx.doi.org/10.1029/2007JF000927.
Muto, M., Furaya, M., 2013. Surface velocities and ice-front positions of eight major glaciers in the Southern Patagonian Ice Field, South America, from 2002 to 2011. Remote Sens. Environ. 139. http://dx.doi.org/10.1016/j.rse.2013.07.034.
Nakawo, M., Iwata, S., Watanabe, O., Yoshida, M., 1986. Processes which distribute supraglacial debris on the Khumbu Glacier, Nepal Himalaya. Ann. Glaciol. 8, 129–131.
Nakawo, M., Yabuki, H., Sakai, A., 1999. Characteristics of Khumbu Glacier, Nepal Himalaya: recent change in the debris-covered area. Ann. Glaciol. 28, 118–122. http://dx.doi.org/10.3189/172756499781821788.
Nicholson, L., Benn, D., 2006. Calculating ice melt beneath a debris layer using meteorological data. J. Glaciol 52 (178), 463–470. http://dx.doi.org/10.3189/172756506781828584.
Nie, Y., Sheng, Y., Liu, Q., Liu, L., Liu, S., Zhang, Y., Song, C., 2017. A regional-scale assessment of Himalayan glacial lake changes using satellite observations from 1990–2015. Remote Sens. Environ. 189, 1–13. http://dx.doi.org/10.1016/j.rse.2016.11.008.
Noh, M.J., Howat, I.M., 2015. Automated stereo-photogrammetric DEM generation at high latitudes: Surface Extraction with TIN-based Search-space Minimization (SETSM) validation and demonstration over glaciated regions. Remote Sens. (52), 198–217. http://dx.doi.org/10.1080/15481603.2015.1008621.
Nuimura, T., Fujita, K., Fukui, K., Asahi, K., Aryal, R., Ageta, Y., 2011. Temporal changes in elevation of the debris-covered ablation area of Khumbu Glacier in the Nepal Himalaya since 1978. Arct. Antarct. Alp. Res. 43 (2), 246–255. http://dx.doi.org/10.1657/1938-4246-43.2.246.
Nuimura, T., Fujita, K., Yamaguchi, S., Sharma, R.R., 2012. Elevation changes of glaciers revealed by multitemporal digital elevation models calibrated by GPS survey in the Khumbu region, Nepal Himalaya, 1992–2008. J. Glaciol. 58 (210), 648–656. http://dx.doi.org/10.3189/2012JoG11J061.
Nuth, C., Kääb, A., 2011. Co-registration and bias corrections of satellite elevation data sets for quantifying glacier thickness change. Cryosphere (5), 271–290. http://dx.doi.org/10.5194/tc-5-271-2011.
Østrem, G., 1959. Ice melting under a thin layer of moraine, and the existence of ice cores in moraine ridges. Geogr. Ann. (41), 228–230. http://dx.doi.org/10.1080/20014422.1959.11907953.
Paul, F., Winsvold, S.H., Kääb, A., Nagler, T., Schwaizer, G., 2016. Glacier remote sensing using Sentinel-2. Part II: mapping glacier extents and surface facies, and comparison to Landsat 8. Remote Sens. 8 (7), 575. http://dx.doi.org/10.3390/rs8070575.
Pementel, S., Flowers, G.E., Schoof, C.G., 2010. A hydrologically coupled higher-order flow-band model of ice dynamics with a Coulomb friction sliding law. J. Geophys. Res. 115. http://dx.doi.org/10.1029/2009JF001621.
Quincey, D.J., Richardson, S.D., Luckman, A., Lucas, R.M., Reynolds, J.M., Hambrey, M.J., Glasser, N.F., 2007. Early recognition of glacial lake hazards in the Himalaya using remote sensing datasets. Glob. Planet. Chang. (56), 137–152. http://dx.doi.org/10.1016/j.gloplacha.2006.07.013.
Reynolds, J.M., Nakawo, M., Raymond, C.F., Fountain, A., 2000. On the formation of supraglacial lakes on debris-covered glaciers. In: Debris-Covered Glaciers. Proceedings of a Workshop held at Seattle, Washington, U.S.A., September 2000, Oxford. vol. 264. IAHS Publication, pp. 153–4161.
Rignot, E., Echelmeyer, K., Krabill, W., 2001. Penetration depth of interferometric synthetic-aperture radar signals in snow and ice. Geophys. Res. Lett. (28), 3501–3504. http://dx.doi.org/10.1029/2000GL012484.
Robertson, C.M., Brook, M.S., Holt, K.A., Fuller, I., Benn, D.I., 2013. Calving retreat and proglacial lake growth at Hooker Glacier, Southern Alps, New Zealand. N. Z. Geogr. (69), 14–25. http://dx.doi.org/10.1111/nzg.12001.
Rounce, D.R., McKinney, D.C., 2014. Debris thickness of glaciers in the Everest area (Nepal Himalaya) derived from satellite imagery using a nonlinear energy balance model. Cryosphere (8), 1317–1329. http://dx.doi.org/10.5194/tc-8-1317-2014.
Rounce, D.R., Watson, C.S., McKinney, D.C., 2017. Identification of hazard and risk for glacial lakes in Nepal Himalaya using satellite imagery from 2000–2015. Remote Sens. 9 (654). http://dx.doi.org/10.3390/rs9070654.
Rounce, D.R., King, O., McCarthy, M., Shean, D.E., Salerno, F., 2018. Quantifying debris thickness of debris-covered glaciers in the Everest region of Nepal through inversion of a sub-debris melt model. J. Geophys. Res. 123. http://dx.doi.org/10.1029/2017JF004395.
Rowan, A.V., Egholm, D.L., Quincey, D.J., Glasser, N.F., 2015. Modelling the feedbacks between mass balance, ice flow and debris transport to predict the response to climate change of debris-covered glaciers in the Himalaya. Earth Planet. Sci. Lett. 430, 427–438. http://dx.doi.org/10.1016/j.epsl.2015.09.004.
Sakai, A., Chikita, K., Yamada, T., 2000. Expansion of a moraine-dammed glacial lake, Tsho Rolpa, in Rolwaling Himal. Nepal Himalaya. Limnology and Oceanography 45, 1401–1408.
Sakai, A., Fujita, K., 2010. Formation conditions of supraglacial lakes on debris-covered glaciers in the Himalayas. J. Glaciol. 56 (195), 177–181. http://dx.doi.org/10.3189/002214310791190785.
Sakai, A., Nishimura, K., Kadota, T., Takeuchi, N., 2009. Onset of calving at supraglacial lakes on debris covered glaciers of the Nepal Himalayas. J. Glaciol. 55 (193), 909–917. http://dx.doi.org/10.3189/002214309790152555.
Sakai, A., Nuimura, T., Fujita, K., Takenaka, S., Nagai, H., Lamsal, D., 2015. Climate regime of Asian glaciers revealed by GAMDAM Glacier Inventory. Cryosphere 9 (3), 865–880. http://dx.doi.org/10.5194/tc-9-865-2015.
Sakakibara, D., Sugiyama, S., 2014. Ice-front variations and speed changes of calving glaciers in the Southern Patagonia Icefield from 1984 to 2011. J. Geophys. Res. Earth Surf. 119, 2541–2554. http://dx.doi.org/10.1002/2014JF003148.
Salerno, F., Guyennon, N., Thakuri, S., Viviano, G., Romano, E., Vuillermoz, E., Cristofanelli, P., Stocchi, P., Agrillo, G., Ma, Y., Tartari, G., 2015. Weak precipitation, warm winters and springs impact glaciers of south slopes of Mt. Everest (central Himalaya) in the last 2 decades (1994–2013). In: The Cryosphere. vol. 9. pp. 1229–1247. http://dx.doi.org/10.5194/tc-9-1229-2015.
Scherler, D., Bookhagen, B., Strecker, M.R., 2011. Spatially variable response of Himalayan glaciers to climate change affected by debris cover. Nat. Geosci. 4, 156–159. http://dx.doi.org/10.1038/ngeo1068.
Shea, J.M., Immerzeel, W.W., Wagnon, P., Vincent, C., Bajracharya, S., 2015. Modelling glacier change in the Everest region, Nepal Himalaya. Cryosphere 9, 1105–1128. http://dx.doi.org/10.5194/tc-9-1105-2015.
Somos-Valenzuela, M.A., Mckinney, D.C., Rounce, D.R., Byers, A.C., 2014. Changes in Imja Tsho in the Mount Everest region of Nepal. Cryosphere (8), 1661–1671. http://dx.doi.org/10.5194/tc-8-1661-2014.
Thakuri, S., Salerno, F., Smiraglia, C., Bolch, T., D'Agata, C., Viviano, G., Tartari, G., 2014. Tracing glacier changes since the 1960s on the south slope of Mt. Everest (central Southern Himalaya) using optical satellite imagery. Cryosphere (8), 1297–1315. http://dx.doi.org/10.5194/tc-8-1297-2014.
Thakuri, A., Salerno, F., Bolch, T., Guyennon, N., Tartari, G., 2016. Factors controlling the accelerated expansion of Imja Lake, Mount Everest region, Nepal. Ann. Glaciol. 57 (71). http://dx.doi.org/10.3189/2016AoG71A063.
Truffer, M., Motyka, R.J., 2016. Where glaciers meet water: subaqueous melt and its relevance to glaciers in various settings. Rev. Geophys. (54), 220–239. http://dx.doi.org/10.1002/2015RG000494.
Trüssel, B., Motyka, R.J., Truffer, M., Larsen, C.F., 2013. Rapid thinning of lake-calving Yakutat Glacier and the collapse of the Yakutat Icefield, southeast Alaska, USA. J. Glaciol. 59 (213). http://dx.doi.org/10.3189/2013J0G12J081.
Tsutaki, S., Sugiyama, S., Sakakibara, D., Sawagaki, T., 2016. Surface elevation changes during 2007–13 on Bowdoin and Tugto Glaciers, northwestern Greenland. J. Glaciol. 62 (236), 1083–1092. http://dx.doi.org/10.1017/jog.2016.106.
Wang, X., Chai, K.G., Liu, S.Y., Wei, J., Jiang, Z., Liu, Q., 2017. Changes of glaciers and glacial lakes implying corridor-barrier effects and climate change in the Hengduan Shan, southeastern Tibetan Plateau. J. Glaciol. 63 (239), 1–8. http://dx.doi.org/10.1017/jog.2017.14.
Warren, C.R., Kirkbride, M.P., 2003. Calving speed and climatic sensitivity of New Zealand lake-calving glaciers. Ann. Glaciol. (36), 173–178. http://dx.doi.org/10.3189/172756403781816446.
Watson, C.S., Quincey, D.J., Carrivick, J.L., Smith, M.W., 2016. The dynamics of supraglacial ponds in the Everest region, central Himalaya. Glob. Planet. Chang. (142), 14–27. http://dx.doi.org/10.1016/j.gloplacha.2016.04.008.
Watson, C.S., Quincey, D.J., Carrivick, J.L., Smith, M.W., 2017. Ice cliff dynamics in the Everest region of the central Himalaya. Geomorphology 278, 238–251. http://dx.doi.org/10.106/j.geomorph.2016.11.017.
Westoby, M.J., Glasser, N.F., Hambrey, M.J., Brasington, J., Reynolds, J.M., Hassan, M.A.A.M., 2014. Reconstructing historic Glacial Lake Outburst Floods through numerical modelling and geomorphological assessment: Extreme events in the Himalaya. In: Earth Surface Processes and Landforms. vol. 39. pp. 1675–1692. http://dx.doi.org/10.1002/esp.3617.

Willis, M.J., Melkonian, A.K., Pritchard, M.E., Ramage, J.M., 2012. Ice loss rates at the Northern Patagonian Icefield derived using a decade of satellite remote sensing. Remote Sens. Environ. 117. http://dx.doi.org/10.1016/j.rse.2011.09.017.

Yamada, T., 1998. Glacier lake and its outburst flood in the Nepal Himalaya, Monograph No. 1, Data Center for Glacier Research. Japanese Society of Snow and Ice, Tokyo, pp. 96.

Yang, X., Zhang, T., Qin, D., Kang, S., Qin, X., 2011. Characteristics and changes in air temperature and Glacier's response on the north slope of Mt. Qomolangma (Mt. Everest). Arctic Antarctic Alpine Res. 43, 147–160. stable/41240408.

Ye, Q., Kang, S., Chen, F., Wang, J., 2006. Monitoring glacier variations on Geladandong mountain, central Tibetan Plateau, from 1969 to 2002 using remote-sensing and GIS technologies. J. Glaciol. 179. http://dx.doi.org/10.3189/172756506781828839.

Zhang, G., Yao, T., Xie, H., Wang, W., Yang, W., 2015. An inventory of glacial lakes in the Third Pole region and their changes in response to global warming. Glob. Planet. Chang. (131), 148–157. http://dx.doi.org/10.1016/j.gloplacha.2015.05.013.